J|A|C|S
ARTICLES

Published on Web 11/16/2009

# Mimicking the Protein Access Channel to a Metal Center: Effect of a Funnel Complex on Dissociative versus Associative Copper Redox Chemistry

Nicolas Le Poul,[†] Bénédicte Douziech,[†] Joceline Zeitouny,[†] Grégory Thiabaud,[‡] Hélène Colas,[†] Françoise Conan,[‡] Nathalie Cosquer,[‡] Ivan Jabin,[§] Corinne Lagrost,[||] Philippe Hapiot,*[,||] Olivia Reinaud,*[,‡] and Yves Le Mest*[,†]

*Laboratoire de Chimie, Electrochimie Moléculaires et Chimie Analytique, CNRS, UMR 6521, Université Européenne de Bretagne à Brest, 6 av. Le Gorgeu, 29238 Brest cedex, France, Laboratoire de Chimie et Biochimie Pharmacologiques et Toxicologiques, CNRS, UMR 8601, Université Paris Descartes, 45 rue des Saints-Pères, 75006 Paris, France, Laboratoire de Chimie Organique, Université Libre de Bruxelles, Brussels, Belgium, and Sciences Chimiques de Rennes, MaCSE, CNRS, UMR 6226, Université Européenne de Bretagne à Rennes 1, Campus de Beaulieu, 35042 Rennes, France*

Received July 8, 2009; E-mail: yves.lemest@univ-brest.fr; olivia.reinaud@parisdescartes.fr; philippe.hapiot@univ-rennes1.fr

***Abstract:*** The control of metal−ligand exchange in a confined environment is of primary importance for understanding thermodynamics and kinetics of the electron transfer process governing the reactivity of enzymes. This study reveals an unprecedented change of the $Cu^{II}/Cu^{I}$ binding and redox properties through a subtle control of the access to the labile site by a protein channel mimic. The cavity effect was estimated from cyclic voltammetry investigations by comparison of two complexes displaying the same coordination sphere (tmpa) and differing by the presence or absence of a calix[6]arene cone surrounding the metal labile site L. Effects on thermodynamics are illustrated by important shifts of $E_{1/2}$ toward higher values for the calix complexes. This is ascribable to the protection of the labile site of the open-shell system from the polar medium. Such a cavity control also generates specific stabilizations. This is exemplified by an impressively exalted affinity of the calixarene system for MeCN, and by the detection of a kinetic intermediate, a noncoordinated DMF guest molecule floating inside the cone. Kinetically, a unique dissymmetry between the $Cu^{I}$ and $Cu^{II}$ ligand exchange capacity is highlighted. At the CV time scale, the guest interconversion is only feasible after reduction of $Cu^{II}$ to $Cu^{I}$. Such a redox-switch mechanism results from the blocking of the associative process at the $Cu^{II}$ state, imposed by the calixarene funnel. All of this suggests that the embedment of a reactive redox metal ion in a funnel-like cavity can play a crucial role in catalysis, particularly for metallo-enzymes associating electron transfer and ligand exchange.

## Introduction

Control of metal−ligand exchange kinetics is a key step in many chemical and biological systems where the change of the redox state of the metal is often interconnected with the modification of the coordination sphere. This is particularly true for copper centers. The $Cu^{I}$ $d^{10}$ ion is relatively indifferent, and hence adaptable, to its environment and readily adopts 3- or 4-coordinate trigonal geometries. In contrast, the $Cu^{II}$ $d^{9}$ ion, due to crystal field and Jahn−Teller effects, has a strong preference for tetragonal environments leading to 4- and 5-coordinate cores.[1,2] As a result, in the absence of sterical hindrance, $Cu^{II}$ exerts a strong electronic/geometric influence on its surroundings. Conversely, in the presence of geometrical constraints such as a trigonal environment, highly energized so-called entatic states can be obtained.[3] The functionality of most copper proteins and enzymes is based on the $Cu^{II}/Cu^{I}$ redox process. Hence, the correlation between the coordination modes of Cu in the protein and the associated electronic properties is a very important target for fundamental and biomimetic purposes.[2,3] Besides the (anchoring) coordination sphere (N-, O-, S-ligands) appending from the protein backbones surrounding the Cu active site, which defines its properties (redox potential, reactivity, ...), an additional labile site is often present.[4]

[†] Université Européenne de Bretagne à Brest.
[‡] Université Paris Descartes.
[§] Université Libre de Bruxelles.
[||] Université Européenne de Bretagne à Rennes 1.

(1) (a) Hathaway, B. J. *Struct. Bonding (Berlin)* **1984**, *57*, 55–118. (b) Solomon, E. I.; Szilagyi, R. K.; George, S. D.; Basumallick, L. *Chem. Rev.* **2004**, *104*, 419–458.
(2) Rorabacher, D. B. *Chem. Rev.* **2004**, *104*, 651–697.
(3) (a) Le Poul, N.; Campion, M.; Izzet, G.; Douziech, B.; Reinaud, O.; Le Mest, Y. *J. Am. Chem. Soc.* **2005**, *127*, 5280–5281. (b) Le Poul, N.; Campion, M.; Douziech, B.; Rondelez, Y.; Le Clainche, L.; Reinaud, O.; Le Mest, Y. *J. Am. Chem. Soc.* **2007**, *129*, 8801–8810. (c) Chaka, G.; Sonnenberg, J. L.; Schlegel, H. B.; Heeg, M. J.; Jaeger, G.; Nelson, T. J.; Ochrymowycz, L. A.; Rorabacher, D. B. *J. Am. Chem. Soc.* **2007**, *129*, 5217–5227.
(4) (a) Kaim, W.; Rall, J. *Angew. Chem., Int. Ed.* **1996**, *35*, 43–60. (b) Messerschmidt, A.; Huber, R.; Poulos, T.; Wieghardt, K. *Handbook of Metalloproteins*; Wiley: New York, 2001. (c) Karlin, K. D.; Tyeklàr, Z. *Bioinorganic Chemistry of Copper*; Chapman & Hall: New York, London, 1993.

 **10.1021/ja9055905 CCC: $40.75** © **2009 American Chemical Society**

In the case of enzymes, it is the reactive site where the substrate and product interact with the metal after passing through the access channel from the external medium. For type 1 proteins devoted to "pure" electron transfer, the control of ligation strength of the axial site trapped in the protein matter is of the most importance. In this case, the labile ligand, often a methionine residue, displays a high affinity for the $Cu^{I}$ state and not for $Cu^{II}$ but remains in the Cu environment.[5] Hence, the control of the labile site by a confined environment, like in a protein chamber, is of primary importance for understanding thermodynamics and kinetics of the electron transfer process that governs the reactivity for enzymes and efficiency/directionality for blue proteins.

Despite this important issue, few studies have been dedicated to the effect of the embedment in a protecting pocket of the [Cu−L] moiety where Cu represents the metal and its coordination sphere and L is a labile ligand. A number of studies have been devoted to the effect of encapsulation of a redox probe on the pure electron transfer process.[6] However, to our knowledge, none of the redox systems described so far presented a modification of its coordination core associated with the electron exchange. In contrast, the strategy consisting of tuning the proximal environment of open-shell complexes by the introduction of various substituents has been largely developed. For example, a number of studies related to Cu complexes embedded in the half-open coordination core provided by the tris(pyridylmethyl)amine (tmpa) $N_4$ donor have evidenced very interesting effects on the redox potentials. However, they generally remain difficult to rationalize because many factors are involved.[7−10] Here, we highlight a unique control, in different respects, of the $Cu^{II}/Cu^{I}$ properties when the metal ion is embedded in a tmpa cap connected to a funnel: the calix[6]arene cone. The cavity effect was directly estimated from cyclic voltammetry (CV) investigations by comparison of two complexes, $[Cu^{II}(calix[6]tmpa)(L)]^{2+}$ and $[Cu^{II}(tmpa)(L)]^{2+}$. These complexes display the same first coordination sphere (tmpa) and only differ by the presence or absence of the calix[6]arene macrocycle surrounding the metal labile site L (Figure 1).[11] The covalent capping of the calixarene macrocycle by a tmpa unit induces a rigid enforcement of the Cu coordination sphere thanks to a strong chelate effect and a well-defined cone conformation.[11,12] Hence, this is an interesting model to study the comparative behavior of two copper redox centers within the same coordinating core, one displaying a labile site freely accessible to the external medium, while the labile site is separated by a funnel-like pocket from the external medium in the second one, similarly to what is effected by a protein chamber.

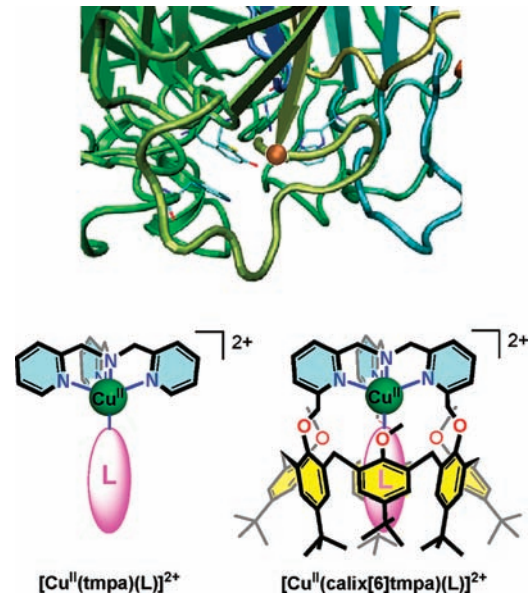


***Figure 1.*** Schematic representations of the $[Cu(tmpa)(L)]^{2+}$ and $[Cu(calix[6]tmpa)(L)]^{2+}$ complexes (L = $H_2O$, MeCN, DMF). Top: Embedded Cu center in the active site of a copper protein (galactose oxidase, PDB code: 1GOF).

## Results and Discussion

**Redox Behaviors of $[Cu^{II}(tmpa)(L)]^{2+}$ and $[Cu^{II}(calix[6]tmpa)(L)]^{2+}$ Complexes in Pure Solvents L = MeCN or DMF.** The Cu complexes have been synthesized as their perchlorate salts according to previously reported procedures.[7c,11b] As previously shown, both complexes display a TBP geometry with a solvent molecule as a fifth ligand (L) in axial position. Upon reduction in pure MeCN or DMF, both complexes show reversible CVs for all investigated scan rates ($0.02 < v < 10$ V $s^{-1}$). This indicates that, in these conditions, the axial ligand, L = MeCN or DMF, remains coordinated to the metal independently of the redox state of the metal, $Cu^{II}$ or $Cu^{I}$. However, the two systems differ by their half-wave potentials for $[Cu^{II/I}(calix[6]tmpa)(L)]^{2+/+}$ and $[Cu^{II/I}(tmpa)(L)]^{2+/+}$: $E_{1/2} = -0.25$ and $-0.62$ V in DMF (L = DMF) and 0.05 and $-0.40$ V in MeCN (L = MeCN) ($E$ vs $Fc^{+}/Fc$), respectively. Easier reduction in MeCN than in DMF can be explained by a better stabilization of the $Cu^{II}$ state by the stronger $\sigma$-donor DMF ligand and of the $Cu^{I}$ state by the $\pi$-acceptor MeCN. Remarkably, the redox potentials are drastically positively shifted by $\Delta E_{1/2} = 370-450$ mV in

(5) (a) Gray, H. B.; Malmström, B. G.; Williams, R. J. P. *J. Biol. Inorg. Chem.* **2000**, *5*, 551–559. (b) George, S. D.; Basumallick, L.; Szilagyi, R. K.; Randall, D. W.; Hill, M. G.; Nersissian, A. M.; Valentine, J. S.; Hedman, B.; Hogdson, K. O.; Solomon, E. I. *J. Am. Chem. Soc.* **2003**, *125*, 11314–11328. (c) Li, H.; Webb, S. P.; Ivanic, J.; Jensen, J. H. *J. Am. Chem. Soc.* **2004**, *126*, 8010–8019. (d) Choi, M.; Sukumar, N.; Liu, A.; Davidson, V. L. *Biochemistry* **2009**, *48*, 9174–9184. (e) Lancaster, K. M.; Yokoyama, K.; Richards, J. H.; Winkler, J. R.; Gray, H. B. *Inorg. Chem.* **2009**, *48*, 1278–1280. (f) Harrison, M. D.; Dennison, C. *ChemBioChem* **2004**, *5*, 1579–1581.
(6) (a) Podkoscielny, D.; Gadde, S.; Kaifer, A. E. *J. Am. Chem. Soc.* **2009**, *131*, 12876–12877, and references cited therein. (b) Sobransingh, D.; Kaifer, A. E. *Chem. Commun.* **2005**, 5071–5073. (c) Stone, D. L.; Smith, D. K.; McGrail, P. T. *J. Am. Chem. Soc.* **2002**, *124*, 856–864.
(7) (a) Karlin, K. D.; Hayes, J. C.; Juen, S.; Hutchinson, J. P.; Zubieta, J. *Inorg. Chem.* **1982**, *21*, 4108–4109. (b) Lim, B. S.; Holm, R. H. *Inorg. Chem.* **1998**, *37*, 4898–4908. (c) Tyeklár, Z.; Jacobson, R. R.; Wei, N.; Murthy, N. N.; Zubieta, J.; Karlin, K. D. *J. Am. Chem. Soc.* **1993**, *115*, 2677–2689. (d) Fox, S.; Nanthakumar, A.; Wikström, M.; Karlin, K. D.; Blackburn, N. J. *J. Am. Chem. Soc.* **1996**, *118*, 24–34.
(8) (a) Chuang, C.-L.; Lim, K.; Chen, Q.; Zubieta, J.; Canary, J. W. *Inorg. Chem.* **1995**, *34*, 2562–2568. (b) Chuang, C.-L.; Lim, K.; Canary, J. W. *Supramol. Chem.* **1995**, *5*, 39–43. (c) Chuang, C.-L.; dos Santos, O.; Xu, X.; Canary, J. W. *Inorg. Chem.* **1997**, *36*, 1967–1972.
(9) Nagao, H.; Komeda, N.; Mukaida, M.; Suzuki, M.; Tanaka, K. *Inorg. Chem.* **1996**, *35*, 6809–6815.
(10) Kunishita, A.; Kubo, M.; Ishimaru, H.; Ogura, T.; Sugimoto, H.; Itoh, S. *Inorg. Chem.* **2008**, *47*, 12032–12039.
(11) (a) Thiabaud, G.; Guillemot, G.; Schmitz-Afonso, I.; Colasson, B.; Reinaud, O. *Angew. Chem., Int. Ed.* **2009**, *48*, 7383–7386. (b) Izzet, G.; Zeng, X.; Akdas, H.; Marrot, J.; Reinaud, O. *Chem. Commun.* **2007**, 810–812. (c) Darbost, U.; Sénèque, O.; Li, Y.; Bertho, G.; Marrot, J.; Rager, M.-N.; Reinaud, O.; Jabin, I. *Chem.-Eur. J.* **2007**, *13*, 2078–2088.
(12) (a) Izzet, G.; Rager, M.-N.; Reinaud, O. *Dalton Trans.* **2007**, 771–780. (b) Izzet, G.; Douziech, B.; Prangé, T.; Tomas, A.; Jabin, I.; Le Mest, Y.; Reinaud, O. *Proc. Natl. Acad. Sci. U.S.A.* **2005**, *102*, 6831–6836. (c) Jabin, I.; Reinaud, O. *J. Org. Chem.* **2003**, *68*, 3416–3419.

***Scheme 1.*** Potential Scale Representing the Effect of the Presence or Absence of the Calix[6]arene Funnel on the Redox Potential

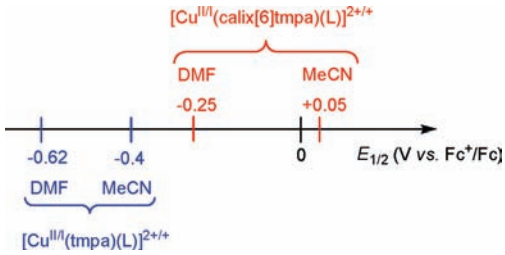


both solvents, when switching from the "simple" tmpa core to calix[6]tmpa (Scheme 1).

Such a potential shift has already been reported with *N-ortho*-pyridyl phenyl-substituted Cu(tmpa) complexes ($\Delta E_{1/2}$ = 300−480 mV).[8] The origin of the shift resulting from a stabilization of the $Cu^{II}$ state was difficult to rationalize due to the geometrical changes of the $Cu^{II}$ state from TBP to SBP upon substitution of the pyridyl *ortho*-position. It has been proposed that the potential shift could originate from multiple effects: electronic, steric/geometric, decrease of the local polarity, variation of the ionic strength... For example, electrodonating substituents in the *para*-position have been shown to exert an expected negative shift.[13] However, with bulky substituents in the ortho position, the negative shift is compensated by steric effects affecting the geometry at the metal center, thus inducing a positive shift.[9] Interestingly, in the case of the calix[6]arene capped by tmpa, the geometrical constrain imposed by the macrocycle leads to nitrilo complexes that remain in a TBP geometry for both oxidation states, just like the unsubstituted tmpa ligand. This is illustrated by the comparison of the XRD structures of $[Cu^{I}(tmpa)(MeCN)]^{+}$ and $[Cu^{II}(tmpa)(MeCN)]^{2+}$,[7,8] to $[Cu^{II}(calix[6]tmpa)(MeCN)](ClO_4)_2$,[11b] displayed in Figure 2 (corresponding structural parameters are reported in Table 1). In solution, the similarity of the geometry is further confirmed

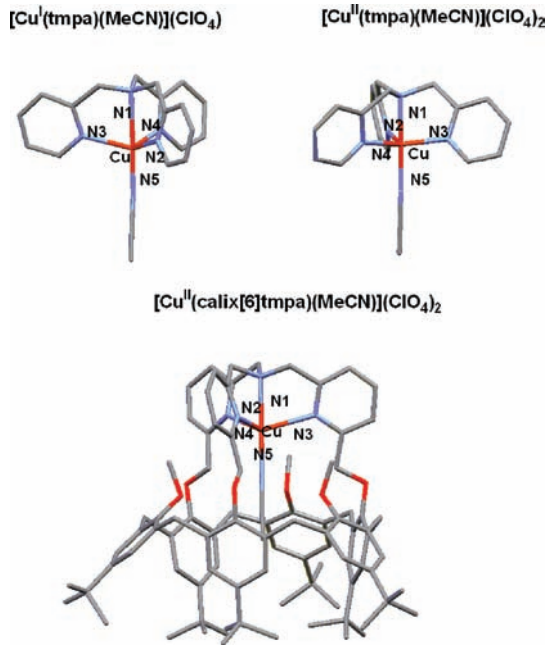


***Figure 2.*** XRD structures of the perchlorato complexes $[Cu^{I}(tmpa)(MeCN)]^{+}$, $[Cu^{II}(tmpa)(MeCN)]^{2+}$, and $[Cu^{II}(calix[6]tmpa)(MeCN)]^{2+}$ from refs 7b, 8, 11b. Hydrogen atoms, counteranions, and solvent of crystallization are omitted for clarity.

***Table 1.*** Selected Bond Distances (Å), Angles (deg), and $\tau$ Values[15] for the Perchlorato Complexes $[Cu^{I/II}(tmpa)(MeCN)]^{n+}$ and $[Cu^{II}(calix[6]tmpa)(MeCN)]^{2+}$ from References 8, 11b[a]

| | $[Cu^{I}(tmpa)(MeCN)]^{+}$ | $[Cu^{II}(tmpa)(MeCN)]^{2+}$ | $[Cu^{II}(calix[6]tmpa)(MeCN)]^{2+}$ |
|---|---|---|---|
| Cu−N(1) | 2.43(1) | 2.104(2) | 2.203(5) |
| Cu−N(2) | 2.08(1) | 2.074(2) | 2.300(6) |
| Cu−N(3) | 2.12(1) | 2.057(2) | 2.301(6) |
| Cu−N(4) | 2.07(1) | 2.033(2) | 2.381(5) |
| Cu−N(5) | 1.99(1) | 1.967(2) | 1.916(5) |
| N(1)−Cu−N(5) | 179.5(5) | 178.3(1) | 176.0(2) |
| $N(1)-Cu-N(2,3,4)_{av}$ | 74.9(1) | 82.14(9) | 75.2(1) |
| $\tau$ values | 1.03 | 0.96 | 0.96 |
| $g$ [$A(10^{-4}$ cm$^{-1}$)] | | $g_{\|\|}$ = 2.0147 (65)* | $g_{\|\|}$ = 1.998 (97) |
| | | $g_{\perp}$ = 2.1921 (113)* | $g_{\perp}$ = 2.182 (75) |
| $\lambda_{max}$ (nm) [$\varepsilon$($M^{-1}$ cm$^{-1}$)] | | 889 (238)* | 830 (470) |

[a] UV−vis−NIR ($CH_2Cl_2$, 293 K) and EPR values ($CH_2Cl_2$, 100 K) data for the perchlorato complexes $[Cu^{II}(tmpa)(L)]^{n+}$ and $[Cu^{II}(calix[6]tmpa)(L)]^{n+}$.[11b] "*": Determined in the present work in the same condition for comparison.

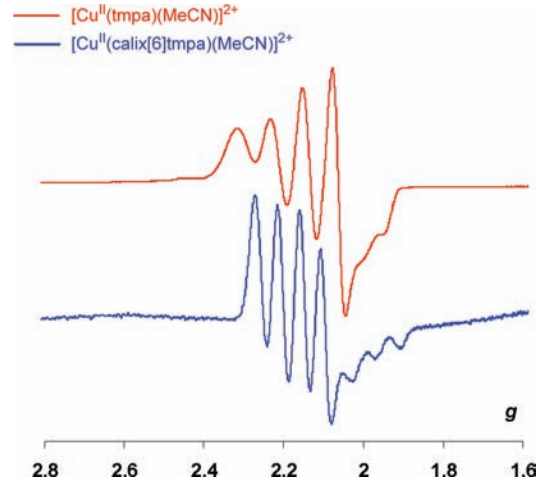


***Figure 3.*** EPR spectra at $T$ = 150 K of frozen solutions of $[Cu^{II}(tmpa)(MeCN)]^{2+}$ (red line)* and $[Cu^{II}(calix[6]tmpa)(MeCN)]^{2+}$ (blue)[11b] in MeCN (*: determined in the present work in the same conditions for comparison).

by similar EPR signatures with $g_{\perp} > g_{||}$ and electronic absorptions that are characteristic of TBP geometries (Table 1 and Figure 3). Finally, variable-temperature $^1$H NMR studies have shown that the $[Cu^{I}(calix[6]tmpa)(MeCN)]^{+}$ complex displays a $C_{3v}$ symmetrical pattern at room temperature that becomes $C_3$ at low $T$, consistent with a rigid TBP geometry.[14]

Hence, geometrical differences between the tmpa- and calixtmpa-based systems cannot account for the large redox shifts observed. Substitutions in *ortho*-position by the moderately electron-rich $CH_2OAr(^tBu)$ calix units are not expected to exert a strong electronic effect. In any case, more electron-donating groups (here $CH_2OAr(^tBu)$ vs H) rather contribute to a negative

(13) Zhang, C. X.; Kaderli, S.; Costas, M.; Kim, E.-I.; Neuhold, Y.-M.; Karlin, K. D.; Zuberbühler, A. D. *Inorg. Chem.* **2003**, *42*, 1807–1824.

(14) Such a phenomenon is evidenced by the diastereo-differentiation of the protons belonging to the wrapping arms and to the aromatic units of the receptors (Izzet, G. Ph.D. Thesis, Paris XI University, defended Dec. 14, 2004). It is classically observed when the calix-host of the funnel complex is filled by MeCN or any other organic ligand larger that CO or $H_2O$. See, for example: (a) Blanchard, S.; Rager, M.-N.; Duprat, A. F.; Reinaud, O. *New J. Chem.* **1998**, 1143–1146. (b) Sénèque, O.; Rondelez, Y.; Le Clainche, L.; Inisan, C.; Rager, M.-N.; Giorgi, M.; Reinaud, O. *Eur. J. Inorg. Chem.* **2001**, 2597–2604, and ref 12a.

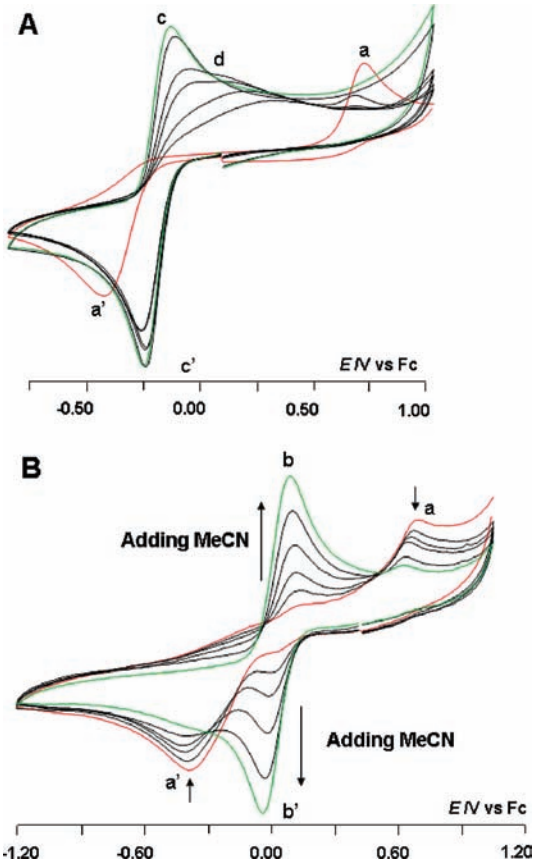


***Figure 4.*** Cyclic voltammograms at a Pt electrode in $CH_2Cl_2/NBu_4PF_6$ 0.1 M ($v$ = 0.1 V $s^{-1}$) of $[Cu^{II}(calix[6]tmpa)(H_2O)]^{2+}$ ($10^{-3}$ M) with progressive addition of (A) DMF, [DMF] = 0 (red) to 0.19 M (green); (B) MeCN, from 0 (a trace) to ca. 0.001 M. See text for the assignment of peaks a−d.

shift,[13] opposite to what is observed. The likely explanation lies in the isolating effect of the calixarene cone from the solvent. Indeed, MeCN as well as DMF are highly polar solvents, which better stabilize dicationic species ($Cu^{II}$−L) relative to monocationic species ($Cu^{I}$−L). Such a solvent effect, which is important for the tmpa system that is half-open to the solvent, is obviously attenuated by the presence of the calixarene macrocycle wrapping the metal labile site. Therefore, it is proposed that the important shifts of $E_{1/2}$ toward higher values observed for the calixarene-based system are mainly due to the exclusion of the [Cu---L] moiety from the polar ionic medium. All of these observations highlight the important effect that a hydrophobic funnel-shaped cavity can have on the thermodynamic properties of a system presenting an exchangeable site.

**Redox Behavior of the $[Cu^{II}(tmpa)(L)]^{2+}$ and $[Cu^{II}(calix[6]tmpa)(L)]^{2+}$ Complexes in $CH_2Cl_2$ before (L = $H_2O$) and upon Progressive Additions of MeCN or DMF.** When synthesized in a noncoordinating solvent, both $Cu^{II}$ complexes present a water molecule in the axial position.[9,11a] In $CH_2Cl_2$, $[Cu^{II}(tmpa)(H_2O)]^{2+}$ displays a reversible process upon reduction for $v >$ 0.2 V $s^{-1}$, corresponding to a fast $H_2O$ unbinding−binding process.[16] Under the same conditions, the reduction of $[Cu^{II}(calix[6]tmpa)(H_2O)]^{2+}$ is electrochemically irreversible (Figure 4A, peak a′) and is followed by $H_2O$ ejection leading to an empty cavity complex $[Cu^{I}(calix[6]tmpa)(Ø)]^{+}$. This empty cavity complex, which has been previously characterized by NMR spectroscopy,[11a] is oxidized at $E_{pa}$ = 0.75 V (Figure 4, peak a). The $H_2O$ ejection occurring after the $Cu^{II}$ reduction is very fast as the reversible peak could never be evidenced at scan rates up to 10 V $s^{-1}$.

Progressive addition of DMF or MeCN (Figure 4A and B) into a $CH_2Cl_2$ solution of the complex leads to the final appearance of a reversible CV corresponding to $[Cu^{II/I}(calix[6]tmpa)(L)]^{2+/+}$ (L = MeCN and DMF, respectively). However, the evolution of the CVs is completely different in each case. In the case of L = MeCN (Figure 4B), from the very first and after each substoichiometric addition of MeCN, the reversible couple $[Cu^{II/I}(calix[6]tmpa)(MeCN)]^{2+/+}$ (peaks b/b′) grows to the detriment of the two irreversible systems $[Cu^{II}(calix[6]tmpa)(H_2O)]^{2+}$ and $[Cu^{I}(calix[6]tmpa)(Ø)]^{+}$ (peaks a′/a). After addition of 1 equiv of MeCN, peaks a′/a have disappeared, and only peaks b/b′ corresponding to the $[Cu^{II/I}(calix[6]tmpa)(MeCN)]^{2+/+}$ couple are observed, thus attesting to the quantitative formation of the MeCN−$Cu^{II}$ complex. Such an impressive affinity for the MeCN guest was also noticed during the NMR characterization of the $Cu^{I}$ complex for which, at millimolar concentrations in a noncoordinating solvent, the presence of 1 equiv of MeCN was enough to feed 100% of the calixarene cavity.[11a] With L = DMF (Figure 4A), the evolution of the CVs appears somewhat more complicated. Indeed, for low to intermediate DMF concentrations, the CVs show the complete disappearance of the $[Cu^{II}(calix[6]tmpa)(H_2O)]^{2+}$ reduction (peak a′), concomitantly with the disappearance of the "empty cavity" peak (peak a). At the same time, the gradual development of two anodic peaks at −0.22 V (peak c associated with its reversible peak c′) and 0.02 V (peak d) is observed. The peaks c/c′, whose intensity increases with the quantity of added DMF, are clearly identified to the $[Cu^{II/I}(calix[6]tmpa)(DMF)]^{2+/+}$ reversible couple, as it is observed in the pure DMF solvent. While the unidentified peak d is not present in the absence of DMF, it disappears by merging with peak c at the highest concentrations of added DMF (>127 mol equiv vs Cu). Peak d cannot be due to the oxidation of species like $[Cu^{I}(calix[6]tmpa)(H_2O)]^{+}$, because the total irreversibility of peak a′ in pure $CH_2Cl_2$ attests to a fast, irreversible, and total ejection of $H_2O$ after the reduction of $[Cu^{II}(calix[6]tmpa)(H_2O)]^{2+}$. Thus, even if $[Cu^{I}(calix[6]tmpa)(H_2O)]^{+}$ existed, it would display a too short lifetime to account for the observed behavior. Moreover, simulations of the voltammograms when only considering the oxidation of $[Cu^{I}(calix[6]tmpa)(DMF)]^{+}$ in equilibrium with the "empty cavity" species do not allow one to reproduce the appearance of the "extra" peak d. Consequently, peak d must correspond to the oxidation of a new species that could be evidenced in the presence of DMF. As it is neither the final $[Cu^{I}(calix[6]tmpa)(DMF)]^{+}$ product nor the empty cavity complex $[Cu^{I}(calix[6]tmpa)(Ø)]^{+}$, we propose this intermediate to be $[Cu^{I}(calix[6]tmpa)(DMF)_{nc}]^{+}$, a complex where the DMF molecule is already inside the cavity, but with no coordination link to the metal center as shown in Scheme 2 (see the Supporting Information). The oxidation potential of such a species is indeed expected to be intermediate between those of $[Cu^{I}(calix[6]tmpa)(DMF)]^{+}$

(15) Addison, A. W.; Rao, T. N.; Reedjik, J.; van Rijn, J.; Verschoor, C. G. *J. Chem. Soc., Dalton Trans.* **1984**, 1349–1356.

(16) At scan rates $v < 0.2$ V $s^{-1}$, the CV behavior denotes the existence of the follow-up reaction between $[Cu^{I}(tmpa)]^{+}$ and $CH_2Cl_2$ leading ultimately to the formation of $[Cu^{II}(tmpa)(Cl)]^{+}$ as indicated by electrolysis. This reaction has been described previously: ref 7c and (a) Lucchese, B.; Humphreys, K. J.; Lee, D.-H.; Incarvito, C. D.; Sommer, R. D.; Rheingold, A. L.; Karlin, K. D. *Inorg. Chem.* **2004**, *43*, 5987–5998. (b) Jacobson, R. R.; Tyeklár, Z.; Karlin, K. D. *Inorg. Chim. Acta* **1991**, *181*, 111–118.

***Scheme 2.*** Ladder Mechanism for $H_2O$−DMF Exchange in the $[Cu^{II/I}(calix[6]tmpa)(L)]^{2+/+}$ Process[a]

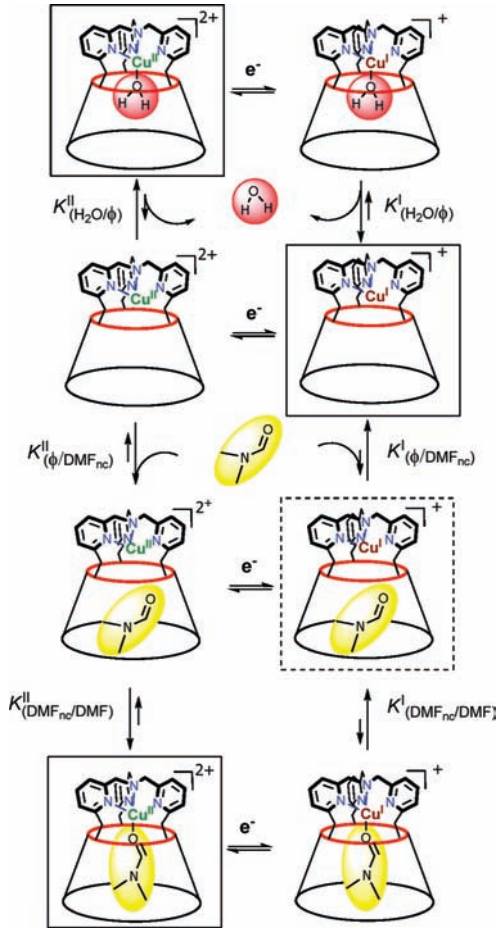

[a] Plain rectangles depict species that have been spectroscopically characterized. The dashed rectangle depicts the kinetic intermediate evidenced by CVs of Figure 4. For each thermodynamic equilibrium constant $K^I$ or $K^{II}$, the associated kinetic constants are $k^I_f/k^I_b$ and $k^{II}_f/k^{II}_b$, respectively (see Supporting Information Scheme S1).

and $[Cu^I(calix[6]tmpa)(Ø)]^+$. It is noticeable that a similar intermediate has been previously evidenced on the basis of a VT NMR study with a closely related calix[6]tren−$Cu^I$ system.[12a] To enforce this hypothesis, numerical simulations (Digisim) have been performed on the basis of a ladder mechanism with the four redox couples displayed in Scheme 2, $[Cu^{II/I}(calix[6]tmpa)(DMF)]^{2+/+}$, $[Cu^{II/I}(calix[6]tmpa)(DMF)_{nc}]^{2+/+}$, $[Cu^{II/I}(calix[6]tmpa)(H_2O)]^{2+/+}$, and $[Cu^{II/I}(calix[6]tmpa)(Ø)]^{2+/+}$. Using a reasonable set of kinetic and thermodynamic parameters, some have been determined previously by UV−vis spectrophotometry,[11b] the mechanism of Scheme 2 allowed us to reproduce the experimental variations with a reasonable agreement considering the number of unknown parameters (see the Supporting Information). On the contrary, this was not possible when not taking into account the existence of the proposed intermediate. Such type of noncoordinated species has already been evidenced on the basis of a VT NMR study with the closely related $[Cu^I(calix[6]tren)]^+$ system.[12a] However, studies related to the encapsulation of noncoordinated guests into the calix[6]arene cavity have shown that the relative stability of the host−guest adducts depends on the polarization of the calixarene receptor at the small rim.[17] The higher is the positive charge, the stronger are the charge (calix)/dipole(guest)-stabilizing interactions. With $Cu^I$ complexes, these noncoordinating adducts are not stable enough to be accumulated at room temperature and remain very difficult to evidence, even at lower temperatures. In the present case, our attempts to trap the DMF intermediates failed. Actually, we were not even capable of accumulating the coordinated species $[Cu^I(calix[6]tmpa)(DMF)]^+$ under the experimental conditions imposed by the NMR technique (5 mM of complex + up to 50 molar equiv of DMF), which just reflects the poor affinity of $Cu^I$ for O-donors. In this connection, cyclic voltammetry appears as a complementary and useful technique due to the fact that the present observation took advantage of kinetics effects. During the CV scan, after reduction of $[Cu^{II}(calix[6]tmpa)(DMF)]^{2+}$, the chemical steps are not at equilibrium. As depicted in Scheme 4, after reduction of $[Cu^{II}(calix[6]tmpa)(DMF)]^{2+}$ to $[Cu^I(calix[6]tmpa)(DMF)]^+$, at low DMF concentrations, there is a fast decoordination step leading to the empty cavity complex, $[Cu^I(calix[6]tmpa)(Ø)]^+$, which is the thermodynamically stable species at the $Cu^I$ redox state in agreement with our NMR observations. Increasing the DMF concentration makes the $Cu^I$−DMF reassociation possible and faster during the consumption of the $Cu^I$ species at the electrode, which displaces the chemical steps (reverse scan). Thus, the detection of the intermediate $[Cu^I(calix[6]tmpa)(DMF)_{nc}]^+$ depends on the competition between the reassociation kinetics rate and the experimental time corresponding to the CV scan rate. During the reverse CV scan, if the reassociation is not totally completed before the applied potential becomes higher than the oxidation potential of $[Cu^I(calix[6]tmpa)(DMF)_{nc}]^+$, the peak corresponding to the direct oxidation of this species is observed (low DMF concentration). For the highest DMF concentrations, the reassociation step becomes so fast that it permits the $Cu^I$ oxidation at the potential of $[Cu^I(calix[6]tmpa)(DMF)]^+$, and only one peak is observed during the reverse scan.[18] All of these observations confirm that $[Cu^I(calix[6]tmpa)(DMF)_{nc}]^+$ is a kinetic transient intermediate, which cannot be accumulated for spectroscopic characterization. This is an unprecedented electrochemical observation for these systems.

**Redox Interconversion of the Axial Ligand.** To obtain more details about the effects of the calix[6]arene cone on the kinetics and thermodynamics of guest exchange reactions inside the cavity, a comparative electrochemical study of both tmpa and calix[6]tmpa $Cu^{II}$ complexes was performed in the presence of different mixtures of competitive ligands, MeCN, and DMF.

**$[Cu^{II/I}(tmpa)(L{\leftrightarrow}L')]^{2+/+}$ Process.** Upon successive additions of MeCN (up to 4.9 M) into a $CH_2Cl_2$/DMF solution of $[Cu^{II}(tmpa)(DMF)]^{2+}$ ([DMF] = 4.5 M), the redox potential of the reversible $Cu^{II/I}$ process gradually shifts toward positive values up to $E_{1/2} = -0.45$ V (Figure 5A). The plot of $E_{1/2}$ versus log([MeCN]) shows an almost linear variation with a slope close to 58 mV/log([MeCN]), for MeCN concentrations ranging from 0.5 to 4.9 M. All of these observations are consistent with a

(17) For host-(noncoordinated) guest adducts with calix[6]arenes polarized by $Zn^{II}$ at the small rim, see: Darbost, U.; Sénèque, O.; Li, Y.; Bertho, G.; Marrot, J.; Rager, M.-N.; Reinaud, O.; Jabin, I. *Chem.-Eur. J.* **2007**, *13*, 2078–2088. For calix[6]arenes polarized by a polyammonium core at the small rim, see: Darbost, U.; Giorgi, M.; Hucher, N.; Jabin, I.; Reinaud, O. *Supramol. Chem.* **2005**, *17*, 243–250. Darbost, U.; Rager, M.-N.; Petit, S.; Jabin, I.; Reinaud, O. *J. Am. Chem. Soc.* **2005**, *127*, 8517–8525.

(18) The subsequent reaction from the noncoordinated $[Cu^I(calix[6]tmpa)(DMF)_{nc}]^+$ to the coordinated $[Cu^I(calix[6]tmpa)(DMF)]^+$ is expected to be rapid.

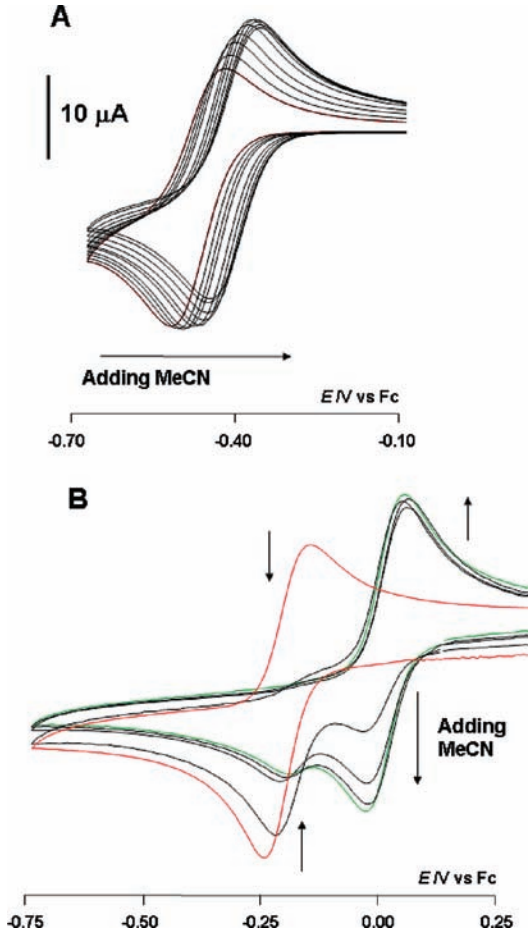


***Figure 5.*** CVs at a Pt electrode in $CH_2Cl_2/NBu_4PF_6$ 0.1 M ($v$ = 0.1 V $s^{-1}$) of (A) $[Cu^{II}(tmpa)(H_2O)]^{2+}$ ($10^{-3}$ M) + DMF (4.5 M) and (B) $[Cu^{II}(calix[6]tmpa)(H_2O)]^{2+}$ ($10^{-3}$ M) + DMF (0.19 M) with progressive addition of MeCN: (A) [MeCN] = 0 to 4.9 M; (B) [MeCN] = 0 (red) to 1.86 M (green).

***Scheme 3.*** Simplified Square Scheme Mechanism Proposed for the DMF−MeCN Ligand Exchange for the $[Cu^{II/I}(tmpa)(L)]^{2+/+}$ and $[Cu^{II/I}(calix[6]tmpa)(L)]^{2+/+}$ Processes in $CH_2Cl_2/NBu_4PF_6$, 0.1 M

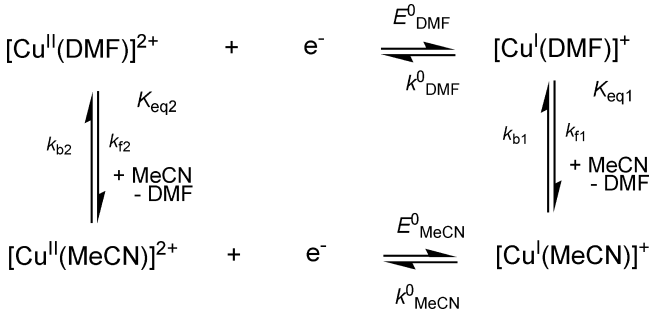


thermodynamic control of the electron transfer (Nernst law) associated with a fast reversible ligand exchange reaction.[19]

Such a situation could be analyzed according to a global square scheme, proposed in Scheme 3, depending on three parameters, the standard potentials $E^0_{DMF}$, taken here as $E_{1/2}$ values before MeCN addition, and the two corresponding thermodynamic equilibrium constants $K_{eq1}$ and $K_{eq2}$ that characterize the chemical equilibria relative to ligand L exchanges for the $Cu^I$ and $Cu^{II}$ redox states. $K_{eq1}$ and $K_{eq2}$ could be estimated as $35 < K_{eq1} < 40$ and $0.05 < K_{eq2} < 0.5$ (see the Supporting Information). The error on $K_{eq2}$ is larger, but the electrochemical estimation agrees with the UV−vis−NIR spectroscopy value ($K_{eq2} = 0.06$). Concerning the equilibrium kinetics, the reversibility of the square scheme conditions shows that the global equilibrium is kinetically fast and thus does not provide more information about the nature of the individual reaction. From simulations of the experimental voltammograms and considering the determined thermodynamic parameters, the lower kinetic limit was estimated as $k_{f1} > 10^3$ $M^{-1}$ $s^{-1}$. Globally, this corresponds to a classical nernstian behavior with a full thermodynamic control with no kinetic limitation.

**$[Cu^{II/I}(calix[6]tmpa)(L{\leftrightarrow}L')]^{2+/+}$ Process.** As shown in Figure 5B, successive additions of MeCN aliquots into a $CH_2Cl_2$/DMF solution of $[Cu^{II}(calix[6]tmpa)(DMF)]^{2+}$ (added [DMF] = 0.19 M) led to a completely different electrochemical situation. Contrarily to the above-described classical situation with the $[Cu^{II}(tmpa)(L)]^{2+}$ complex, the addition of MeCN does not lead to a shift of the half-wave potential, but instead, to the progressive decrease of the $[Cu^{II}(calix[6]tmpa)(DMF)]^{2+}$ reduction peak at $E_{pc} = -0.24$ V with a concomitant increase of a new reversible system at $E_{1/2} = 0.05$ V, both systems interconverting instead of shifting. Interestingly, from the first addition of MeCN, the $[Cu^{II/I}(calix[6]tmpa)(DMF)]^{2+/+}$ couple becomes irreversible, and only the $[Cu^I(calix[6]tmpa)(MeCN)]^+$ peak is detected on the reverse scan. After addition of 10 equiv of MeCN relative to DMF, almost only one reversible system remains at $E_{1/2} = 0.05$ V corresponding to the reversible $[Cu^{II/I}(calix[6]tmpa)(MeCN)]^{2+/+}$ process. Moreover, for all MeCN additions, the variation, $i_p$ with $v^{1/2}$, of the $[Cu^{II}(calix[6]tmpa)(MeCN)]^{2+}$ reduction peak current, $E_{pc} \approx 0.0$ V, is linear. The intensity, therefore, reflects the initial quantity of $[Cu^{II}(calix[6]tmpa(MeCN)]^{2+}$ present in solution before the start of the scan and shows that the ligand interconversion $[Cu^{II}(DMF){\leftrightarrow}Cu^{II}(MeCN)]$ in the $Cu^{II}$ species does not occur, through a CE process in the diffusion layer, on the time scale of the CV experiment.[20] This indicates that the interconversion equilibrium between the DMF and MeCN complexes is completely blocked (frozen equilibrium)[19] at the level of this electrochemical process. A second observation concerns the complete irreversibility of the second cathodic peak, at $E_{pc} = -0.24$ V, corresponding to the reduction of $[Cu^{II}(calix[6]tmpa)(DMF)]^{2+}$ that becomes totally irreversible from the first addition of MeCN and remains irreversible even at the highest available scan rate ($v$ = 1 V $s^{-1}$), that is, for the shortest available experimental time. It shows that (i) the equilibrium for the $Cu^I$ redox state is completely shifted toward $[Cu^I(calix[6]tmpa)(MeCN)]^+$ ($K_{eq1}$ very high) and that (ii) the transformation from the DMF to the MeCN complex is extremely fast at the $Cu^I$ state contrarily to the $Cu^{II}$ state for which the ligand exchange is frozen. The behavior of the $[Cu^{II/I}$-

(19) Savéant, J.-M. *Elements of Molecular and Biomolecular Electrochemistry*; Wiley-Interscience: Hoboken, NJ, 2006.

(20) This first peak could be analyzed with the formalism of the CE mechanism (a chemical step "C" followed by an electron transfer "E"). Yet, with $[Cu^{II/I}(tmpa)calix(DMF{\leftrightarrow}MeCN)]^{2+/+}$, the interconversion equilibrium $Cu^{II}(DMF){\leftrightarrow}Cu^{II}(MeCN)$ is too slow to be displaced by the consumption of $Cu^{II}(MeCN)$ during the CV scan (so called "frozen equilibrium"). An opposite situation would have been a very fast ligand exchange equilibrium. In such a case, as soon as the reduction of the $Cu^{II}(MeCN)$ into $Cu^I(MeCN)$ begins, all $Cu^{II}$ (L = DMF or L = MeCN) would be reduced thanks to a fast displacement of the interconversion equilibrium near the electrode surface. In that kinetics situation, only one reduction peak would have been observed. This situation corresponds to the behavior previously observed with $[Cu^{II/I}$-$(tmpa)(DMF{\leftrightarrow}MeCN)]^{2+/+}$, when the complex did not contain the calixarene macrocycle.

***Scheme 4.*** Comparative Mechanisms Proposed for the Electrochemically Driven Interchange of Axial Ligand between the $[Cu^{II/I}(tmpa)(DMF{\leftrightarrow}MeCN)]^{2+/+}$ and $[Cu^{II/I}(calix[6]tmpa)(DMF{\leftrightarrow}MeCN)]^{2+/+}$ Processes

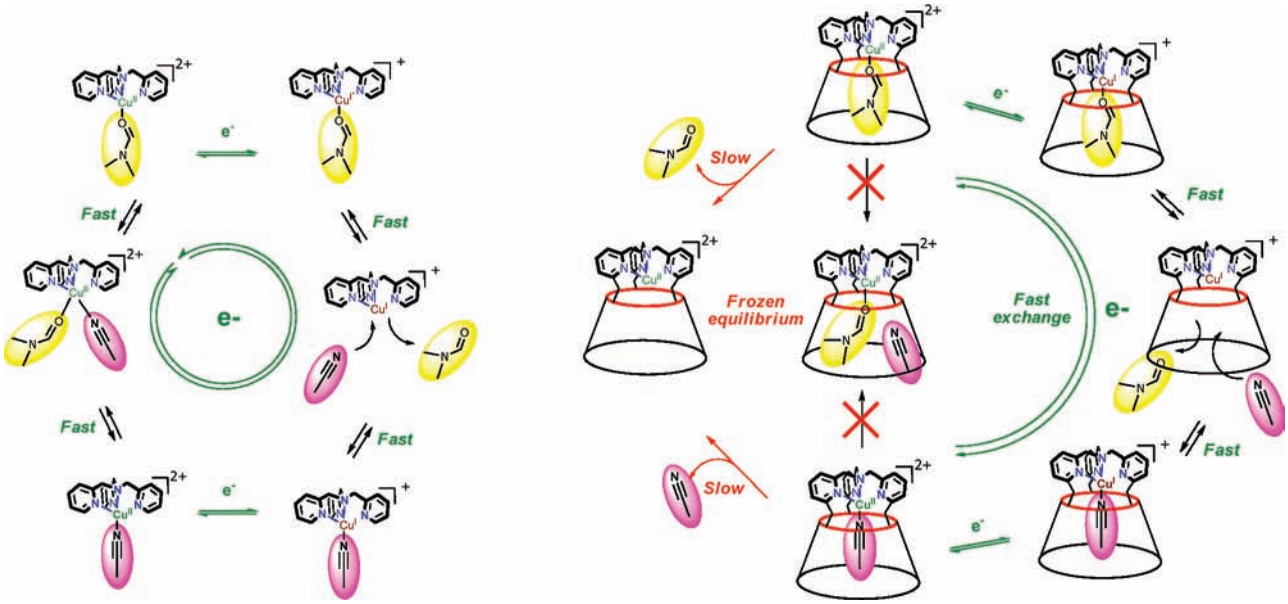


$(calix[6]tmpa)(L)]^{2+/+}$ process seriously contrasts with that of $[Cu^{II/I}(tmpa)(L)]^{2+/+}$, for which all ligand exchanges, at the $Cu^{II}$ or $Cu^{I}$ state, are found to be fast. The limiting mechanism for ligand exchange is either associative or dissociative. It is generally suggested that five-coordinate $Cu^{II}$ complexes display an associative character (due to the high Lewis acidity of $Cu^{II}$ and the crystal field in such a trigonal environment), in contrast to $Cu^{I}$ that more likely undergoes dissociative exchange.[21] The associative mechanism implies that the departure of the coordinated ligand only occurs once the new guest has arrived. As proposed in the comparative Scheme 4, this situation is very likely the case for the tmpa complexes for which one axial ligand site is free to access. Conversely, it is obvious that the presence of the calix[6]arene funnel makes the associative mechanism impossible as two ligands cannot simultaneously bind the metal center inside the cavity at the level of the small rim. As a result, only dissociative type ligand exchanges are possible within the funnel.[11b] Thus, at the $Cu^{I}$ level, the exchange process is fast with or without cavity, in full agreement with a dissociative mechanism.[22] In contrast, the fact that the exchange process at the $Cu^{II}$ level is fast in the absence of a cavity and "frozen" within a cavity is evidence of a different mechanism for each complex. It is clearly dissociative within the cavity due to the hindrance imposed by the calix[6]tmpa ligand. However, due to the high Lewis acidity of the $Cu^{II}$ center, this dissociative ligand exchange is too slow to be detected at the CV time scale. In the case of tmpa without cavity, the exchange is associative and fast due to the facile approach of the competitive ligand. As a result, and as illustrated in Scheme 4, in the case of the tmpa complex, the $Cu^{II}/Cu^{I}$ redox process responds thermodynamically to the composition of the medium with absolutely no kinetic limitation: the process always remains fully reversible with a potential evolving in a nernstian way as a function of the concentration. Conversely, the protected site controls the ligand exchange through the blocking effect of any associative process. It generates a very specific behavior, which emphasizes the role of the surrounding funnel at the redox level. The behavior is no more nernstian, and the $Cu^{II}$ redox site does not respond to the composition of the solution, but only to the guest ligand present inside the cavity before the beginning of the CV experiment. As long as the reduction into $Cu^{I}$ does not occur, the ligand exchange, even if thermodynamically favorable, remains unfeasible (see Scheme 4). To this extent, the reduction process constitutes a redox switch for the "activation" of the interaction between the substrate/ligand present in the external medium.

## Conclusion

In conclusion, this study sheds light on the remarkable effects that a cavity controlling the access to the metal has on the metal binding and redox behavior. The control of the surrounding of the axial metal site generates specific stabilization exemplified here by an impressively exalted affinity of the calixarene system for MeCN, and by the detection on the CV time scale of a noncoordinated DMF guest. Both observations are directly attributable to the supramolecular effect of the cavity respectively by enforcing the [Cu−MeCN] interaction in one case and by generating DMF−cavity host−guest weak interactions in the second case. On the basis of the present results, it seems also that the noticeable effect on the control of the redox potential of the $Cu^{II}/Cu^{I}$ process could be ascribed to a shielding of the labile ligand site [Cu−L] from the external medium, a consequence that had been evocated before, but never discriminated.[7−10] Undoubtedly, the most impressive effect concerns the unique dissymmetry between the $Cu^{I}$ and $Cu^{II}$ ligand exchange capacity, that is, fast against slow exchange created by the embedment of the metal into the calixarene. Contrarily to the complex based on the simple tmpa core, the overall redox potential of the cavity-embedded system [Cu(calix[6]tmpa)] does not respond to the composition of the solution through rapid equilibrium: the ligand exchange is only feasible after reduction of the $Cu^{II}$ complex. The reduction step to $Cu^{I}$ thus appears as a redox switch, which opens the way to guest interconversion. This blocking effect of the associative process, and its implications,

(21) (a) Neubrand, A.; Thaler, F.; Körner, M.; Zahl, A.; Hubbard, C. D.; Van Eldik, R. *J. Chem. Soc., Dalton Trans.* **2002**, 957–961. (b) Hubbard, C. D.; Van Eldik, R. *J. Coord. Chem.* **2007**, *60*, 1–51.
(22) Rondelez, Y.; Rager, M.-N.; Duprat, A.; Reinaud, O. *J. Am. Chem. Soc.* **2002**, *124*, 1334–1340.

has never been unraveled in the $Cu^{II}/Cu^{I}$ redox chemistry to the best of our knowledge. Thus, it seems that this is clearly a valuable effect for the complete understanding of the redox behavior of cavitand systems such as obviously Cu enzymes. This is true not only for the thermodynamic and kinetic control of the redox process as established here, but also must be true, intuitively and speculatively at the moment, for the understanding of the reactivity. For example, during the catalytic cycles involving $O_2$ activation by mono copper (mono)oxygenases, which is an extremely hot topic, the first step involves the reduction/decoordination of the $Cu^{II}-L$ resting state to allow the initiating $Cu^{I}-O_2$ interaction. As a hydroxylated product is formed and transiently bound to $Cu^{II}$, to get turnovers, the enzyme must again address the two concurrent features: $Cu^{II}$ reduction/product expulsion. Hence, our study suggests that, for metallo-enzymes associating electron transfer and ligand exchange, the embedment of the labile site of the reactive redox metal ion in a funnel-like cavity may well play a crucial role in catalysis.

## Experimental Section

**Chemicals.** The tris(2-pyridylmethyl)-amine ligand (tmpa) was synthesized as previously described by reaction of 2 equiv of chloromethylpyridinium with 1 equiv of 2-aminomethylpyridine in aqueous NaOH solution for 72 h.[7c] The corresponding $Cu^{II}$ complex, $[Cu^{II}(tmpa)(H_2O)]^{2+}$, either as a perchlorate or as a triflate salt, was prepared according to the previously described procedure.[23] The (calix[6]tmpa) ligand and $[Cu^{II}(calix[6]tmpa)(H_2O)](ClO_4)_2$ complex were prepared as previously reported.[11]

(23) Jacobson, R. R.; Tyeklár, Z.; Karlin, K. D.; Zubieta, J. *Inorg. Chem.* **1991**, *30*, 2035–2040.

**Electrochemical and Spectroscopic Experiments.** The electrochemical studies of the copper complexes have been performed in a glovebox (Jacomex) ($O_2 < 1$ ppm, $H_2O < 1$ ppm) with a home-designed three-electrodes cell (WE, Pt; RE, Ag; CE, Pt). The potential of the cell was controlled by an AUTOLAB PGSTAT 100 (Ecochemie) potentiostat monitored by a computer. Anhydrous dimethylformamide (99.9% Sigma-Aldrich), "extra-dry" dichloromethane ($H_2O < 30$ ppm, Acros), and acetonitrile (99.9% BDH, VWR) were used as received and kept under $N_2$ in the glovebox. The supporting salt, $NBu_4PF_6$, was purified, dried under vacuum for 48 h at 100 °C, then kept under $N_2$ in the glovebox. All experiments have been performed with solutions of ca. 0.001 M in electroactive species and 0.1 M in $NBu_4PF_6$. UV−vis−NIR spectroscopy was performed with a JASCO V-670 spectrophotometer.

Numerical simulations of the voltammograms were performed with the BAS DigiSim simulator 3.03 (BAS DigiSim Simulation Software for Cyclic Voltammetry), using the default numerical options with the assumption of planar diffusion and a Butler−Volmer law for the electron transfer. The charge-transfer coefficient, $\alpha$, was taken as 0.5.

**Acknowledgment.** This research was supported by CNRS and Agence National pour la Recherche (Calixzyme Project ANR-05-BLAN-0003). Conseil Régional de Bretagne is thanked for a doctoral grant for J.Z.

**Supporting Information Available:** CV experiments, simulations, kinetics, and thermodynamics values; information about the procedure and estimations of the parameters. This material is available free of charge via the Internet at http://pubs.acs.org.

JA9055905